

Distribution of the distance between opposite nodes of random polygons with a fixed knot

¹Akihisa Yao, ²Hiroshi Tsukahara, ³Tetsuo Deguchi and ¹Takeo Inami

¹Department of Physics, Faculty of Science and Engineering,
Chuo University, 1-13-27 Kasuga, Bunkyo-ku, Tokyo 112-8551

²Geographic Information Systems Department,
Hitachi Software Engineering Co., Ltd.
4-12-7 Higashishinagawa, Shinagawa-ku, Tokyo 140-0002

³Department of Physics,
Faculty of Science, Ochanomizu University
2-1-1 Ohtsuka, Bunkyo-ku, Tokyo 112-8610

March 9, 2004

Abstract

We examine numerically the distribution function $f_K(r)$ of the distance r between opposite polygonal nodes for random polygons with a fixed knot type K . Here we consider some knots such as \emptyset , 3_1 and $3_1\#3_1$. In a wide range of r , the shape of $f_K(r)$ is well fit to the scaling form [1] derived from the field theory for self-avoiding walks. The fit yields the exponents $\nu_K = \frac{1}{2}$ and $\gamma_K = 1$, which are consistent with the exponents of the Gaussian distribution. We also introduce a fitting formula to the distribution $g_K(R)$ of the gyration radius R for random polygons under some topological constraint K . It is significant for the form of the distribution whether random polygons have a topological constraint or not.

1 Introduction

Polymer chains in solutions or gels may be highly self-entangled: such entanglements should be important to understand some features of polymeric materials. A variety of knots can appear by linking the two ends of a polymer chain. In fact, various knotted DNAs are synthesized in

experiments through random closure of nicked DNA chains [2, 3]. Since topological questions were put forward by Delbrück, Frisch and Wasserman [4, 5], several aspects of knotted ring polymers have been studied numerically and analytically such as the probability of random knotting [6–15], the average sizes [16, 17] and the complexity of their conformations [18].

Let us discuss the average size of knotted ring polymers with no excluded volume, i.e., the mean-squared gyration radius $R_K^2(N)$ of N -noded random polygons with a fixed knot type K [19–25]. We consider random polygons as a simple model of ring polymers in solution at the θ -point [26]. In fact, ring polymers at the θ -point should have no effect of excluded volume but keep their topology unchanged. It has now been established in the simulations [20, 22–24] that the average size of random polygons with a fixed knot is larger than that of no topological constraint, when N is large enough. The topological swelling of random polygons may be explained in terms of entropic repulsion caused by the topological constraint. The phenomenon should be closely related to the “topological excluded volume” proposed for such random polygons that possess the trivial knot \emptyset [19]. Concerning the large- N behavior of $R_K^2(N)$, however, the numerical studies do not unanimously arrive at the same conclusion. We have analyzed the data of $R_K^2(N)$ for a model of random polygons [23], assuming the scaling formula in the following:

$$R_K^2(N) = A_K N^{\nu_K} (1 + B_K N^{-\Delta_K} + \dots) . \quad (1)$$

The result is quite favorable to the interpretation of $\nu_K = \nu_{\text{SAW}}$, however, it can also be consistent with $\nu_K = \nu_{\text{RW}}$. Here, self-avoiding walks (SAW) and random walks (RW) have the scaling exponent $\nu_{\text{SAW}} = 0.588$ and $\nu_{\text{RW}} = 0.5$, respectively. It seems that it is nontrivial to determine the asymptotic exponent ν_K numerically. Furthermore, even other possibilities have not been completely excluded, yet. It would thus be interesting to investigate some other quantity related to the large- N behavior of random polygons having the same knot.

In this paper we discuss the following two quantities for random polygons with a fixed knot: i) the distribution function of the distance between opposite nodes and ii) the distribution of the radius of gyration. If the “topological excluded volume” corresponds to a certain amount of excluded volume, then the distance between opposite nodes should follow a non-Gaussian distribution. For ring polymers with excluded volume, the distribution of the distance between opposite nodes should be non-Gaussian, while it is Gaussian for random polygons. Here we

assume that the distance between opposite polygonal nodes plays the similar role as the end-to-end distance of a linear chain. For the self-avoiding walk, the end-to-end distance distribution is non-Gaussian [27, 28].

Through computer simulation of random polygons with some fixed knots, we have numerically evaluated the distributions of the distance between opposite nodes of random polygons under the topological constraints [29]. The symbols \emptyset , 3_1 , and $3_1\#3_1$ denote the trivial knot, the trefoil knot, and the composite knot consisting of two trefoil knots, respectively. We show that the scaling form gives good fitting curves to the data of the distributions over a wide range of the distance between opposite nodes. The good fit should be quite remarkable. In fact, the scaling form of the end-to-end distance distribution of SAW is derived in a limited range by taking the limit where the length N and the distance r goes to infinity keeping the normalized distance $\rho = r/N^\nu$ finite and very large [1, 27, 28, 30–34].

We have also numerically evaluated the distributions of the gyration radius for random polygons under some topological constraints [29]. We introduce a formula for describing the distributions, and discuss its fitting curves. We thus investigate topological effects on the average sizes of random polygons. The formula of the gyration-radius distribution should be new, in particular, for random polygons under topological constraints. Here we note that there have been several theoretical researches on the distribution of the gyration radius, such as its asymptotic scaling form for the Gaussian chains [35, 36]. Compared to the end-to-end distribution function, however, scaling properties of the gyration-radius distribution have not extensively discussed, yet, either theoretically or even numerically. For instance, it is not known whether there exist connections between a certain asymptotic behavior of the gyration-radius distribution and the critical exponent of a macroscopic quantity.

The content of the paper consists of the following. In §2, we explain the model of random polygons, and define some symbols for the distribution functions. In §3, we describe briefly some procedures of the computer simulation. In §4, we discuss the numerical results of the present research. We plot the distribution functions of the intersegment distance for random polygons under topological constraints, and discuss good fitting curves to them. We also plot the distributions of the gyration radius for random polygons under topological constraints. In

§5, we discuss an open question.

2 Model and distribution functions

We consider a model of random polygons in which a polygon \mathcal{P}_N consists of N line segments of length a and it is specified by position vectors of its nodes, $\mathcal{P}_N = (\mathbf{r}_1, \mathbf{r}_2, \dots, \mathbf{r}_N)$. All cyclic permutations of the set of position vectors correspond to the same polygon. We recall that random polygons have no excluded volume. Hereafter we set $a = 1$.

When a polygon is topologically equivalent to a knot K , we call it a polygon of knot type K . The configuration space \mathcal{C} of polygons is divided into subspaces \mathcal{C}_K in which all polygons have the same knot K . We have $\mathcal{C} = \sum_K \mathcal{C}_K$.

For a polygon \mathcal{P}_N , we denote the intersegment vector from the i th node to the $i + \lambda N$ th node

$$\mathbf{r}(i; \lambda, \mathcal{P}_N) = \mathbf{r}_{i+\lambda N} - \mathbf{r}_i, \quad (2)$$

where the progress parameter λ takes a value between 0 and 1. Here we assume the convention: $\mathbf{r}_{N+i} = \mathbf{r}_i$.

We define the distribution of the distance between the i th and the $i + \lambda N$ th nodes by the probability $f(r; \lambda, N)\Delta r$ that the length of the intersegment vector $\mathbf{r}(i; \lambda, \mathcal{P}_N)$ takes a value between r and $r + \Delta r$:

$$f(r; \lambda, N)\Delta r = \frac{1}{NM} \sum_{m=1}^M \sum_{i=1}^N \int_r^{r+\Delta r} dr \delta(r - |\mathbf{r}(i; \lambda, \mathcal{P}_{N,m})|). \quad (3)$$

Here Δr is a small positive real number. We choose it so that the statistical fluctuation of $f(r; \lambda, N)$ becomes moderately small. The distribution of the distance between two nodes for random polygons with a fixed knot type K is similarly defined by

$$f_K(r; \lambda, N)\Delta r = \frac{1}{NM_K} \sum_{m=1}^M \sum_{i=1}^N \int_r^{r+\Delta r} dr \delta(r - |\mathbf{r}(i; \lambda, \mathcal{P}_{N,m})|) \chi(\mathcal{P}_{N,m}, K), \quad (4)$$

Here the indicator function $\chi(\mathcal{P}, K)$ filters the polygons of knot type K ; it takes the value 1 if $\mathcal{P} \in \mathcal{C}_K$ and 0 otherwise.

We calculate the distribution $f(r; \lambda, N)$ of the intersegment distance r by randomly generating a large number of polygons $\mathcal{P}_{N,m}$ with length N for $m = 1, \dots, M$. Here the subscript m denotes the m th polygon generated. The number of generated polygons of the knot type K is given by $M_K = \sum_m \chi(\mathcal{P}_{N,m}, K)$, and we have $M = \sum_K M_K$.

Let us denote the square of the gyration radius of a polygon \mathcal{P}_N by

$$R_G^2(\mathcal{P}_N) = \frac{1}{2N^2} \sum_{i,j=1}^N (\mathbf{r}_i - \mathbf{r}_j)^2. \quad (5)$$

We define the distribution $g(R; N)$ for gyration radius R by

$$g(R; N)\Delta R = \frac{1}{M} \sum_{m=1}^M \int_R^{R+\Delta R} dR \delta \left(R - \sqrt{R_G^2(\mathcal{P}_{N,m})} \right), \quad (6)$$

and the one for polygons with knot type K by

$$g_K(R; N)\Delta R = \frac{1}{M_K} \sum_{m=1}^M \int_R^{R+\Delta R} dR \delta \left(R - \sqrt{R_G^2(\mathcal{P}_{N,m})} \right) \chi(\mathcal{P}_{N,m}, K). \quad (7)$$

3 Simulation procedure

A pivot move for a polygon is a rotation of a chain of segments, randomly chosen from the polygon, around the axis passing the two endmost nodes of the chain by a random amount of angle ϕ [23, 37]. The rotation angle ϕ is selected randomly from the interval between 0 and 360 degrees. We do not check self-intersections during the process of rotation of the chain since such configurations are negligible in the space \mathcal{C} .

We start from a seed conformation placed on the cubic lattice, which is regarded as a special conformation of the off-lattice polygon in the continuum space [38]. We then generate a sequence of polygons by applying the pivot moves repeatedly. After discarding the initial 2000 transient conformations, we take samples of polygons at every 200 pivot moves.

To determine the topology of polygons, we employ two simple knot invariants. We calculate the special value of the Alexander polynomial $\Delta_K(t)$ at $t = -1$ [6] (which is also called the determinant of a knot), and the Vassiliev invariant of the second order $v_2(K)$ [39, 40]. With these invariants, the chance of wrong identification of the real topology class for a given polygon

should be negligible and much smaller than the statistical errors of the data, as far as the simple knots are concerned.

The simulation has been performed for polygons with the length $N = 300$ and 600 . We have generated $M = 3 \times 10^6$ random polygons for each given length N . We have classified those polygons into four groups according to their knot types, that is, the three groups of polygons with the specific knot types such as the trivial knot \emptyset , the trefoil knot 3_1 , and the composite knot $3_1 \# 3_1$, together with the group of the knot types other than the previous three knots. Here we note that the three knots have distinct sets of values for the two knot invariants $|\Delta_K(t = -1)|$ and $v_2(K)$.

The distribution function $f_K(r; \lambda, N)$ of the intersegment distance r has been evaluated at the progress parameter $\lambda = 1/4, 1/2$ and $3/4$ for random polygons under some topological constraint K [29]. However, we focus on the case of $\lambda = 1/2$ in the present paper. The other cases will be discussed in a later publication. The range of intersegment distance r is divided into a number of bins of with the width Δr . Here we set $\Delta r = 0.25$. We enumerate the number of intersegment distances in each of the bins. The distribution function is obtained by dividing the number of each bin by the total number of intersegment distances. Similarly we numerically evaluate the distribution $g_K(R; N)$ of gyration radius R for random polygons under some topological constraint K . Here we take $\Delta R = 0.25$.

4 Results of the simulation

4.1 Functional forms of the distributions

The asymptotic scaling form of the end-to-end distance distribution of the self-avoiding walks is derived for the region $\rho \gg 1$ [1,30,31]. However, we now apply it to the data of the distribution function of the distance between opposite nodes for random polygons under some topological

constraint K . We thus have the following:

$$f_K(r; \lambda, N) = A_K r^{2+\theta_K} \exp \left[-D_K r^{\delta_K} \right], \quad (8)$$

$$\theta_K = \frac{d\nu_K + 1 - \gamma_K - d/2}{1 - \nu_K}, \quad (9)$$

$$\delta_K = \frac{1}{1 - \nu_K}. \quad (10)$$

For the distribution $g_K(R; N)$ of gyration radius R , we introduce the following formula:

$$g_K(R; N) = A_{g,K} |R - c_K|^{\theta_{g,K}} \exp \left[-D_{g,K} |R - c_K|^{\delta_{g,K}} \right], \quad (11)$$

where c_K is a constant. We note that Fixman's result [35] corresponds to a special case to the formula (11).

4.2 Distribution function $f_K(r; \lambda, N)$ of intersegment distance r

The intersegment distributions $f_K(r; \lambda, N)$ at $\lambda = 1/2$ for $N = 300$ and 600 are presented in figures 1 and 2, respectively. Here the topological conditions denoted by K correspond to restriction of random polygons into the following sets: (i) all polygons; (ii) polygons of the trivial knot \emptyset ; (iii) polygons of the trefoil knot 3_1 ; (iv) polygons of the composite knot $3_1 \# 3_1$; (v) polygons of any knot types other than the three knots \emptyset , 3_1 , and $3_1 \# 3_1$. We thus consider the five different topological conditions. We note that the case (i) corresponds to no topological constraint. We denote the distribution functions of the five cases simply as f_{all} , f_{\emptyset} , f_{3_1} , $f_{3_1 \# 3_1}$, and f_{others} , respectively.

The fitting curves of figures 1 and 2 are fit well to the data points. The curves are given by the scaling form (8), and are all very close to the Gaussian distributions. Here we note that it is also the case with the data for $\lambda = 1/4$ and $3/4$. The numerical estimates for the exponents θ_K and δ_K and the constants A_K and D_K are given in Tab. 1. The actual ranges of distance r used for the fitting curves are also shown in Tab. 1. The fitting curves fit very well to the data points not only in the range of r larger than the peak position but almost in the entire range of r . The χ^2 values per datum are very small. Very small deviations are only seen in the small r region, although the region is out of the fitting ranges.

The best estimates of the exponents θ_K and δ_K almost agree with the Gaussian values, i.e., $\nu_K \approx 1/2$ and $\gamma_K \approx 1$, within the range of estimation errors for all the five different topological conditions and for each polygon length $N = 300$ and 600 . The constant D_K depends on the length N . However, it does not change very much for the different knot types with respect to the estimation errors. The constant A_K depends on the knot type K for $N = 300$. However, the difference among A_K 's becomes smaller for $N = 600$ than for $N = 300$. It is thus suggested that they should become the same value when N is very large.

Let us denote by r_K the peak position of the distribution $f_K(r)$. Assuming the scaling form (8), the peak position r_K is given by

$$r_K = \left(\frac{2 + \theta_K}{D_K \delta_K} \right)^{1-\nu_K} \quad (12)$$

The peak position r_K may characterize the knot dependence of the distribution function $f_K(r)$. When $\nu_K = 0.5$ and $\gamma_K = 1.0$, the form of $f_K(r)$ is determined by the estimate D_K . Here A_K is derived from the normalization condition.

In figure 1, the peak position r_\emptyset of the distribution $f_\emptyset(r)$ is larger than r_{all} of f_{all} . For f_{others} , r_{others} is smaller than r_{all} . In figure 2, the peak positions of f_\emptyset , f_{3_1} , and $f_{3_1\#3_1}$ are all larger than that of f_{all} for $N = 600$. Their values of $N = 600$ are much closer to each other than in the case of $N = 300$. Here the peak position r_{others} of f_{others} is smaller than that of f_{all} also in the case of $N = 600$. It is thus suggested that when N is very large, the peak positions of $f_K(r)$ of simple knots should be given by the same value and the distributions $f_K(r)$ should approach a universal form.

The observations in figures 1 and 2 in the above also suggest that fixing a knot type of a random polygon cause an effective repulsion or attraction among internal segments of the polygon depending on the complexity of the knot. When the length N becomes very large, polygons of very complex knots can appear. They should have smaller conformations than other polygons of simpler knots. As we see in figure 1 for $N = 300$, random polygons with the trivial knot have larger conformations on the average than those of no topological constraints, while random polygons of more complex knots have smaller conformations.

Let us summarize the results in the subsection. We have found that the distribution $f_K(r; \lambda, N)$ is well fitted by the same functional form as the Gaussian one. However, the position

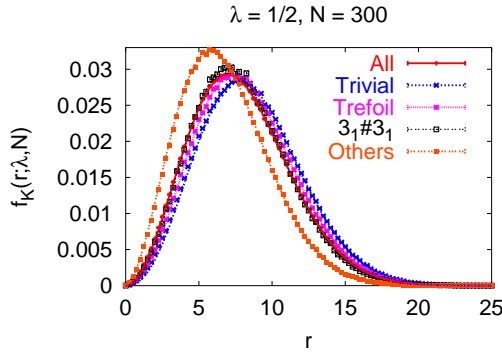


Figure 1: The distributions $f_K(r; \lambda, N)$ of intersegment distance r at $\lambda = 1/2$ and $N = 300$.

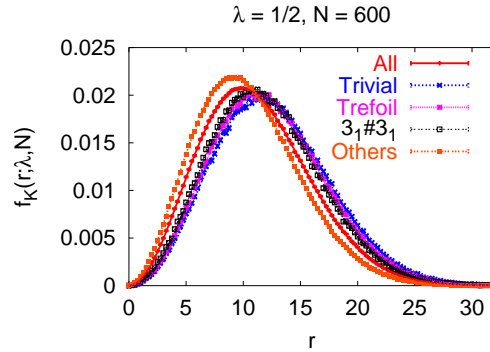


Figure 2: The distributions $f_K(r; \lambda, N)$ of intersegment distance r at $\lambda = 1/2$ and $N = 600$.

of the peak depends on the knot type K . For simple knots such as the \emptyset , 3_1 and $3_1\#3_1$, the peak positions are shifted to larger values than that of the distribution f_{all} of polygons under no topological constraint. This is consistent with the effective swelling observed in the studies on the average sizes of random polygons with some fixed knots [20, 22–24].

4.3 Distribution $g_K(R; N)$ of gyration radius R

The distribution functions $g_K(R; N)$ of gyration radius R are presented in figures 3 and 4 for $N = 300$ and 600 in the five topological conditions. Here the five cases are explained in the previous section. We denote the distributions for the five cases briefly as g_{all} , g_{\emptyset} , g_{3_1} , $g_{3_1\#3_1}$, and g_{others} , respectively.

We have applied the formula (11) to the data points in some ranges of R as shown in table 2. We find in figures 3 and 4 that the fitting curves fit well to the data points in the ranges of R . We therefore consider that the formula (11) approximates the distribution $g_K(R; N)$ of gyration radius effectively, and we can discuss the topological effect with the fitting parameters. However, the formula (11) does not necessarily express the precise functional form of $g_K(R; N)$. The χ^2 values are large in particular for g_{all} and g_{others} . Here we note that the statistical errors of the data points are very small, so that small deviations from the fitting curves can lead to large χ^2

values.

We denote by R_K the peak position of the distribution $g_K(R; N)$ with respect to R . In figure 3, the peak position R_\emptyset of the distribution g_\emptyset is larger than those of the other distributions g_{all} , g_{3_1} , $g_{3_1\#3_1}$ and g_{others} . In figure 4, the peaks of g_\emptyset , g_{3_1} , $g_{3_1\#3_1}$ are clearly located in the right hand side of the peak of g_{all} . The peak of g_{others} is located in the left hand side of the peak of g_{all} . The observations suggest that random polygons of relatively simple knots such as \emptyset , 3_1 and $3_1\#3_1$ are larger in size, and those of complex knots are smaller than the average one. Furthermore, the distributions, g_{all} , g_{3_1} , $g_{3_1\#3_1}$ in figure 4 of $N = 600$ are closer to each other than in figure 3. It is thus suggested that the distribution $g_K(R; N)$ of a knot K should converge to a universal form when N becomes very large.

The best estimates of the exponents $\theta_{g,K}$ and $\delta_{g,K}$ and the constants $D_{g,K}$, $A_{g,K}$ and c_K are given in table 2. For the three knots $K = \emptyset$, 3_1 and $3_1\#3_1$, the exponents $\theta_{g,K}$ and $\delta_{g,K}$ are independent of the knot type both for $N = 300$ and 600 with respect to the errors: $\theta_{g,K} \approx 9.3$ and $\delta_{g,K} \approx 1.12$ for $N = 300$; $\theta_{g,K} \approx 8.6$ and $\delta_{g,K} \approx 1.20$ for $N = 600$. For the case of no topological constraint, however, the exponents $\theta_{g,all}$ and $\delta_{g,all}$ are distinct from those of the three knots. It is thus significant for the form of the gyration-radius distribution of random polygons whether they are under any topological constraint or not. Here we recall that for the distributions $f_K(r; \lambda, N)$, the exponents γ_K and ν_K are independent of the knot type or the topological constraint.

5 Discussions

Let us denote by ν'_K the scaling exponent defined for the asymptotic behavior of the average size of SAW such as given in (1). For SAW, the exponent ν'_K corresponds to the exponent ν_K determined by the formula (8) [1]. If des Cloizeaux's relations (9) and (10) could be valid for random polygons under topological constraints, we should have $\nu'_K \simeq 0.50$ from the best estimates for the distribution $f_K(r; \lambda, N)$ as shown in table 1.

Within the scope of the present research, however, it is not clear whether the two exponents ν_K and ν'_K should be equal or not. Moreover, it is not clear whether the relations (9) and (10) should be valid for random polygons under topological constraints. It seems that the form

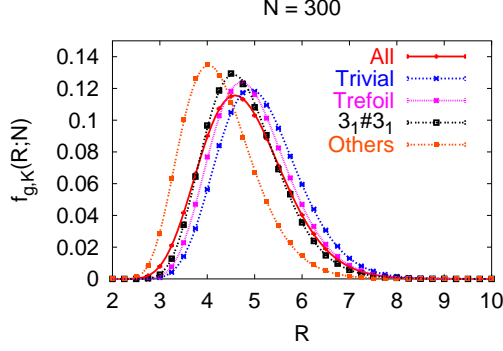


Figure 3: The distribution $g_K(R; N)$ of gyration radius R for $N = 300$.

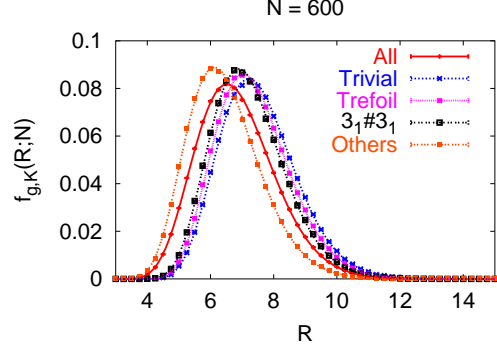


Figure 4: The distribution $g_K(R; N)$ of gyration radius R for $N = 600$.

Table 1: The fitting values of the scaling formula (8) to the data of the distribution $f_K(r; \lambda, N)$ at $\lambda = 1/2$, N and K denote the polygonal length and the topological condition, respectively. The χ^2 value per datum is shown in the column of χ^2 .

N	K	γ_K	ν_K	$D_K \times 10^2$	$A_K \times 10^3$	χ^2	Fitting Range
300	<i>all</i>	1.04 ± 0.03	0.503 ± 0.005	1.9 ± 0.1	1.78 ± 0.09	1.13	5.75 – 20
	\emptyset	0.87 ± 0.13	0.509 ± 0.019	1.7 ± 0.5	0.8 ± 0.1	1.05	6.5 – 16
	3_1	0.93 ± 0.09	0.50 ± 0.01	1.9 ± 0.3	1.1 ± 0.1	0.90	6.25 – 19
	$3_1 \# 3_1$	1.0 ± 0.1	0.51 ± 0.02	2.0 ± 0.6	1.5 ± 0.3	0.85	5.75 – 17
	<i>others</i>	1.1 ± 0.1	0.48 ± 0.02	2.9 ± 0.6	4.0 ± 0.5	0.81	5.5 – 15
600	<i>all</i>	1.03 ± 0.02	0.501 ± 0.004	0.99 ± 0.05	0.63 ± 0.03	0.76	7.5 – 30
	\emptyset	0.8 ± 0.2	0.51 ± 0.03	0.8 ± 0.4	0.19 ± 0.07	0.78	9 – 23
	3_1	0.8 ± 0.2	0.51 ± 0.02	0.9 ± 0.3	0.22 ± 0.06	1.22	8.5 – 23.75
	$3_1 \# 3_1$	1.0 ± 0.1	0.52 ± 0.02	0.7 ± 0.3	0.29 ± 0.06	0.92	7.5 – 22
	<i>others</i>	1.06 ± 0.05	0.493 ± 0.008	1.2 ± 0.1	0.94 ± 0.09	0.97	8.25 – 28.5

Table 2: The fitting values of the formula (11) to the data of the distribution $g_K(R; N)$ of gyration radius. N and K denote the polygonal length and the topological condition, respectively. The χ^2 value per datum is shown in the column of χ^2 .

N	K	$\theta_{g,K}$	$\delta_{g,K}$	$D_{g,K} \times 10^2$	$A_{g,K}$	c_K	χ^2	Fitting Range
300	<i>all</i>	6.6 ± 0.5	1.40 ± 0.05	2.2 ± 0.3	1.2 ± 0.2	1.96 ± 0.05	6.86	2.25 – 9
	\emptyset	9.0 ± 0.5	1.22 ± 0.04	2.0 ± 0.2	2.1 ± 0.2	2.15 ± 0.03	2.88	2 – 9
	3_1	9.3 ± 0.4	1.12 ± 0.03	7 ± 2	2.9 ± 0.3	2.13 ± 0.03	3.61	2 – 9
	$3_1 \# 3_1$	9.6 ± 0.9	1.03 ± 0.06	30 ± 15	3.8 ± 0.7	2.13 ± 0.05	3.03	2 – 9
	<i>others</i>	7 ± 2	1.1 ± 0.1	77 ± 63	3 ± 1	2.0 ± 0.0	13.04	2.25 – 9
600	<i>all</i>	6.4 ± 0.4	1.40 ± 0.04	2.0 ± 0.5	0.7 ± 0.1	2.86 ± 0.07	9.71	3 – 12
	\emptyset	8.5 ± 0.4	1.25 ± 0.04	0.8 ± 0.1	1.26 ± 0.14	3.36 ± 0.04	2.19	3 – 12
	3_1	8.8 ± 0.5	1.18 ± 0.04	1.5 ± 0.3	1.6 ± 0.2	3.32 ± 0.05	4.00	3 – 12
	$3_1 \# 3_1$	8.5 ± 0.4	1.18 ± 0.04	2.3 ± 0.4	1.6 ± 0.2	3.31 ± 0.04	3.16	3 – 12
	<i>others</i>	7.4 ± 0.9	1.17 ± 0.07	8 ± 1	1.6 ± 0.4	2.8 ± 0.1	12.28	3 – 12

of the distribution $f_K(r; \lambda, N)$ remains Gaussian with the exponent $\nu_K \simeq 0.50$ in the limit $N \rightarrow \infty$. However, the average size $R_K^2(N)$ might follow the scaling form with a different exponent, $\nu'_K > 0.5$.

Acknowledgment

The authors are grateful to M. K. Shimamura for helpful discussions. A.Y. was supported in part by the Chuo University.

References

- [1] J. des Cloizeaux. *Phys. Rev. A*, 10:1665–1669, 1974.
- [2] S. Y. Shaw and J. C. Wang. *Science*, 260:533, 1993.

- [3] V.V. Rybenkov N.R. Cozzarelli and A.V. Vologodskii. *Proc. Natl. Acad. Sci. USA*, 90:5307, 1993.
- [4] M. Delbrück. *Proc. Symp. Appl. Math.*, 4:55–63, 1962.
- [5] H. L. Frisch and E. Wasserman. *J. Amer. Chem. Soc.*, 83:3789, 1961.
- [6] A. V. Vologodskii, A. V. Lukashin, M. D. Frank-Kamenetskii, and V. V. Anshelevich. *Sov. Phys. JETP*, 39:1059–1063, 1974.
- [7] J. P. J. Michels and F. W. Wiegel. *Phys. Lett.*, 90A:381–384, 1982.
- [8] J. des Cloizeaux and M. L. Mehta. *J. Physique*, 40:665–670, 1979.
- [9] D. W. Sumners and S. G. Whittington. *J. Phys. A*, 21:1689–1694, 1988.
- [10] N. Pippenger. *Disc. Appl. Math.*, 25:273–278, 1989.
- [11] K. Koniaris and M. Muthukumar. *Phys. Rev. Lett.*, 66:2211–2214, 1991.
- [12] T. Deguchi and K. Tsurusaki. *J. Knot Theory and its Ramifications*, 3:321–353, 1994.
- [13] T. Deguchi and K. Tsurusaki. *Lectures at Knots '96*, ed. S. Suzuki (World Scientific, Singapore):95–122, 1997.
- [14] M. K. Shimamura and T. Deguchi. *J. Phys. Soc. Japan*, 70:1523–1536, 2001.
- [15] A. Dobay, P.-E. Sottas, J. Dubochet, and A. Stasiak. *Lett. Math. Phys.*, 55:239, 2001.
- [16] E. Orlandini, M. Tesi, E. J. Janse van Rensburg, and S. G. Whittington. *J. Phys. A*, 31:5953–5967, 1998.
- [17] M. K. Shimamura and T. Deguchi. *Phys. Rev. E*, 65:051802, 2002.
- [18] M. K. Shimamura and T. Deguchi. *Phys. Rev. E*, 68:061108, 2003.
- [19] J. des Cloizeaux. *J. Physique Lett. (France)*, 42:L433–L436, 1981.
- [20] J. M. Deutsch. *Phys. Rev. E*, 59:R2539–2541, 1999.

- [21] A. Yu. Grosberg. *Phys. Rev. Lett.*, 85:3858, 2000.
- [22] M. K. Shimamura and T. Deguchi. *J. Phys. A*, 35:L241–L246, 2002.
- [23] H. Matsuda, A. Yao, H. Tsukahara, T. Deguchi, K. Furuta, and T. Inami. *Phys. Rev. E*, 68:011102, 2003
- [24] A. Dobay, J. Dubochet, K. Millet, P.E. Sottas, and A. Stasiak. *Proc. Natl. Acad. Sci. USA*, 100:5611–5615, 2003.
- [25] A. Yu. Grosberg. Talk in the conference: Knots, random walks and biomolecules. *in Les Diablerets, Switzerland, July 14–17*, 2003.
- [26] P. G. de Gennes. *Scaling Concepts in Polymer Physics*. Cornell Univ. Pr., New York, 1979.
- [27] M. Bishop and J. H. R. Clarke. *J. Chem. Phys.*, 94:3936–3942, 1991.
- [28] M. Bishop and J. H. R. Clarke. *J. Chem. Phys.*, 95:4589–4592, 1991.
- [29] A. Yao. Topological effects on statistical mechanical properties of ring polymers (in Japanese). *Ph. D Thesis*, Chuo University, 2004.
- [30] M. E. Fisher. *J. Chem. Phys.*, 44:616–622, 1966.
- [31] D.S. McKenzie and M.A. Moore. *J. Phys. A.*, 4:L82–L86, 1971.
- [32] M. Lipkin, Y. Oono, and K. F. Freed. *Macromolecules*, 14:1270–1277, 1981.
- [33] S. Caracciolo, M. S. Causo, and A. Plissetto. *J. Chem. Phys.*, 112:7693–7710, 2000.
- [34] L. Lue and S.B. Kiselev. *J. Chem. Phys.*, 110:2684–2691, 1999.
- [35] M. Fixman. *J. Chem. Phys.*, 36:306–310, 1962.
- [36] H. Yamakawa. *Modern Theory of Polymer Solutions*. Harper & Row, Publishers, New York, 1971.
- [37] J.J. Freire and A. Horta. *J. Chem. Phys.*, 65:4049–4054, 1976.

- [38] A. Yao, H. Matsuda, H. Tsukahara, M. K. Shimamura, and T. Deguchi. *J. Phys. A*, 34:7563–7577, 2001.
- [39] T. Deguchi and K. Tsurusaki. *Phys. Lett. A*, 174:29–37, 1993.
- [40] M. Polyak and O. Viro. *Int. Math. Res. Not.*, (11):445–453, 1994.